Fast neutron dose rate monitoring using off the shelf Helium-4 scintillation detectors

Paolo Tancioni, Rico Chandra, Marco Panniello, Ulisse Gendotti
Arktis Radiation Detectors Ltd
Räffelstrasse 11, 8045 Zürich, Switzerland

Abstract

The capability to measure neutron dose rate with an accuracy of +/- 20% is demonstrated for the helium-4 fast neutron scintillation detector model s670 by Arktis Radiation Detectors. Measurements were performed utilizing quasi-monoenergetic neutron fluxes in an energy range between 0.144 and 14.8 MeV as well as using calibrated Cf-252 and Americium-Beryllium (Am-Be) sources.

The elastic scattering reaction between neutrons and (_^4)He enables detection of neutrons whilst preserving the information about their energy. This measurement technique does not require neutron moderators, resulting in a remarkably lighter configuration. The readings from the detector were plotted against neutron energy to obtain energy calibration curves. Neutron fluence rates measured by certified laboratory detectors were used to calculate intrinsic efficiency values for various irradiation energies.

Fluence per unit dose equivalent factors were used to derive the ambient dose equivalent rate values from the measured neutron energy spectra. The results are used to implement a dose rate calculation in the system software, capable of providing neutron ambient dose equivalent rate values. The accuracy of the computed values is validated with calibrated Cf-252 and Am-Be sources. This work highlights the versatility of such a system, which extends to applications where not only simple neutron counting is required but neutron energy information is also of interest to assess the radiological risk caused by a neutron flux. This system can be used in a variety of applications ranging from dose monitoring in nuclear power plants to risk-assessment of nuclear waste drums coming from the decommissioning of nuclear facilities.

Keywords: neutron; safety; helium-4; dose

1. Introduction

Fast neutrons fluxes are generally coming from sealed radionuclide sources, nuclear power plants, fuel enrichment facilities and particles accelerators. Neutron sources are also used for various industrial purposes.

The major difficulties in detecting fast neutron and measuring their energy arise from the wide energy range a neutron flux can present, the important dependence of the medium cross section with neutron energy and the possible presence of different types of radiation in the same environment, especially gamma rays. The system described in this work, a high-pressure ^{4}He gas scintillation detector model s670 by Arktis Radiation Detectors Ltd, was irradiated with quasi-monoenergetic neutron fluxes ranging from 0.144 to 14.8 MeV. In this region, the most probable interaction of neutrons with light nuclei such as helium is elastic scattering.

He-4-based neutron detection technologies, characterized by higher availability and lower cost of the scintillation gas medium compared to ^{3}He, have been gaining increasing interest as a reliable and affordable neutron detection technology. Moreover, unlike ^{3}He detectors which rely on the absorption of a thermal neutron, ^{4}He detectors exploit excellent fast neutron elastic scattering properties of the gas. This enables the manufacturing of detection systems without utilizing moderators, thus preserving neutron energy information. Using helium-4 as a detection medium, a fast neutron can lose up to around 64% of its initial kinetic energy in a single elastic scattering interaction. This information was used to characterize the detector response at different irradiation energies, allowing to obtain accurate energy calibration curves.

Moreover, helium's low atomic number (Z = 2) results in a low electron density, which reduces the probability of gamma interaction. Additionally, gamma interactions in the active volume generate recoil electrons, which are characterised by low rate of energy deposition. These electrons will be more likely to hit the detector wall before depositing all of its energy. Gamma rays are also characterised by lower light yield in helium scintillation if compared to neutron interactions, which makes this detection technique more advantageous than liquid scintillation detection systems when operating in intense gamma field. In gaseous

helium, these combined effects result in the slow component of the scintillation pulse of a gamma event being up to 8 times smaller than that of a neutron event [1], allowing pulse shape discrimination (PSD).

For neutron spectrometry applications, ^{4}He scintillation techniques have the additional advantage of having an elastic scattering cross section of the scintillation medium which is characterized by a peak for the scattering angle resulting in the maximum energy deposit. This behaviour is not visible for other neutron detection techniques which relies on proton-recoil interactions, being characterized by an elastic scattering cross-section that is almost constant for increasing scattering angles [3].

In this work, pressurized ^{4}He fast neutron scintillation detector model s670 by Arktis Radiation Detectors Ltd is used to implement an ambient dose equivalent rate calculation for dose monitoring purposes, highlighting the possibility to exploit this technology in every environment that is characterized by a high fast neutron radiation component, improving radiological safety of workers.

2. The detection system

Arktis Radiation Detectors model s670 fast neutron detector, shown in figure 1, consists of a stainless-steel tube filled with pressurized ^{4}He, divided into three optically decoupled and identical segments, each containing 8 Silicon Photomultipliers (SiPM) for light collection. The electronic board for signal processing is mounted on one end of the tube, where the TTL output is visible as well.

2.1 Working principle and operational parameters

When fast neutrons interact with helium nuclei through elastic scattering, kinetic energy is transferred from the neutron to the target helium nucleus. The nucleus slows down in the pressurized gas, producing excited and ionized species that de-excite emitting scintillation light.

The 24 SiPMs operating in the s670 fast neutron detector convert the light pulse into an electric signal, which is subsequently processed by the electronic board.

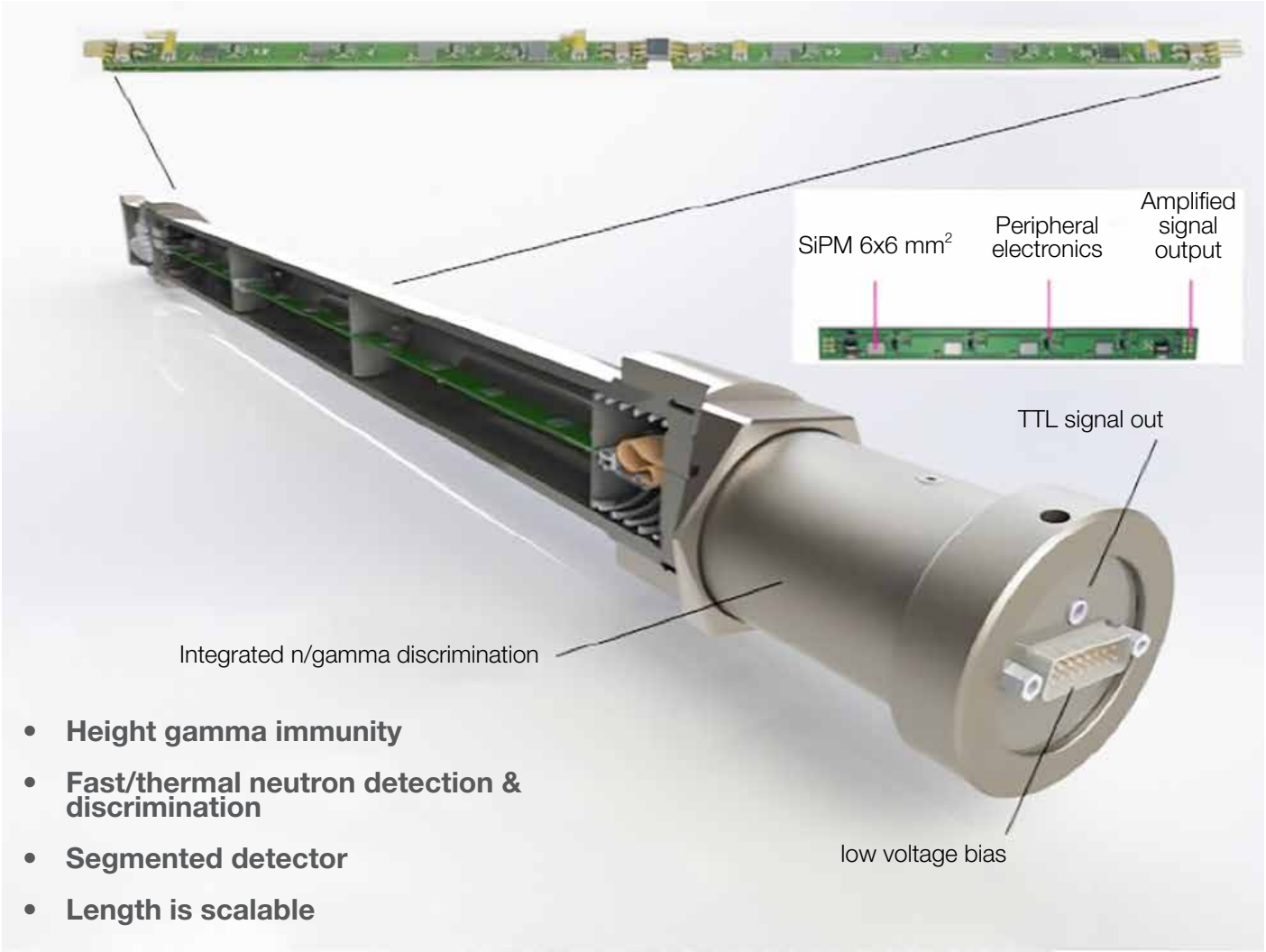

Figure 1: High-pressure He-4 scintillation detector model s670 by Arktis Radiation Detectors Ltd.

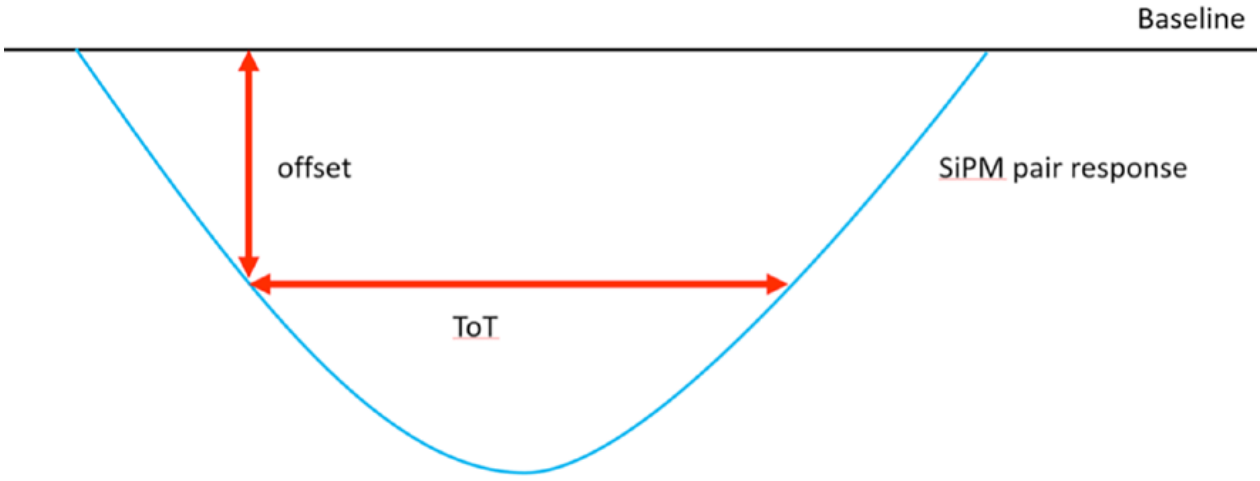

Figure 2: Definition of the parameters “Time-over-Threshold” and “offset”.

The output information of the detector is a Time-over-Threshold (ToT), i.e. the time duration during which the response amplitude of the signal coming from the SiPMs is above a tunable threshold. This electronic threshold is called offset, and it can be adjusted separately for each segment to tailor the sensitivity to the specific application. The offset value is set such that only signals of a certain height are accepted as valid and hence are stored for post analysis. Depending on the value of the ToT signal generated by one event inside the tube, a different TTL signal is produced.

A schematic description of these parameters is shown in Figure 2.

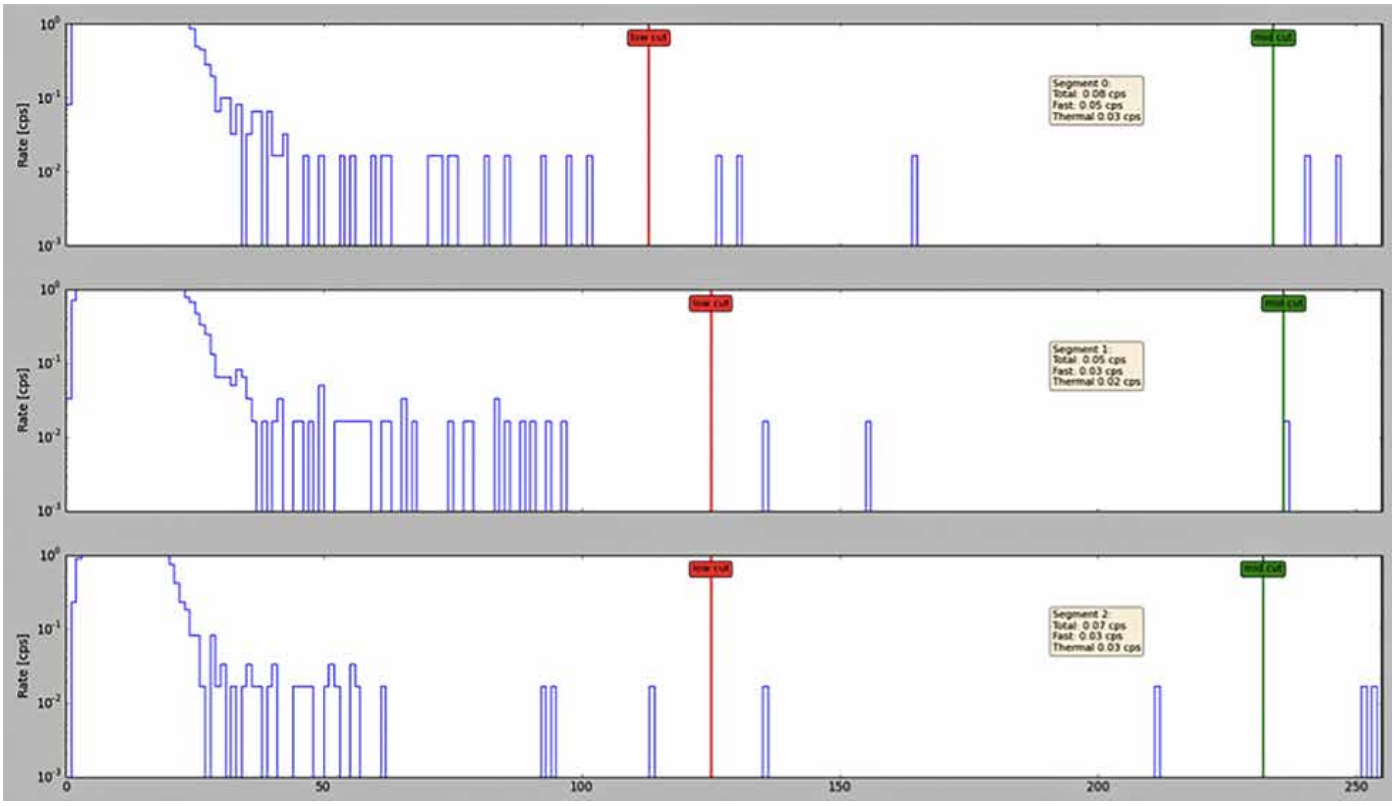

Figure 3: Output histogram showing background count rate versus ToT channel for the three segments of the s670 neutron detector. Different ToT regions are identified by the low-cut (red), mid-cut (green) and high-cut (coinciding with the right end of the x-axis).

Another parameter of importance acting on the ToT histograms is the cut. Applying a “low-cut”, “mid-cut”, and “high-cut” on the ToT signal width, it is possible to define an optimal gamma-rejection ToT region for the detector and to focus on well-defined regions of interest based on the width of the signals that generate counts in those regions.

A typical output of a background measurement reporting count rate versus ToT channel is shown in Figure 3 for each of the three optically decoupled segments. The desired gamma-rejection is set by the low-cut (red), while mid-cut (green) and high-cut (here coinciding with the right end of the x-axis) can be set to focus on a particular ToT region of interest.

3. Measurement campaign

3.1 Irradiation tests with monoenergetic neutron fields

To assess the detector performance for various neutron energies, an extensive experimental campaign was conducted at the neutron irradiation facility (PIAF) at Physikalisch-Technische Bundesanstalt (PTB) in Berlin, Germany [5].

Quasi-monoenergetic neutron fields were utilized to irradiate an array of s670 neutron detectors and acquire data for neutron energies of 0.144, 0.565, 1.2, 2.5, 5, 14.8 MeV.

The measurements took place in a low-scattering measurement hall, where two s670 detectors were positioned at

reaction	target	θ_n	E_n [MeV]	ΔE_n [keV]	ϕsc/ϕdir
^{7}Li(p,n)^{7}Be	LiF 75 µg/cm^2	0°	0.144	12	0.020(5)
^{7}Li(p,n)^{7}Be	LiF 75 µg/cm^2	0°	0.565	8	0.016(4)
^{3}H(p,n)^{3}He	Ti(T) 0.955 mg/cm^2	0°	1.2	74	0.034(8)
^{3}H(p,n)^{3}He	Ti(T) 0.955 mg/cm^3	0°	2.5	52	0.015(4)
^{3}H(d,n)^{4}He	Ti(T) 1.076 mg/cm^4	0°	14.8	434	0.015(4)

Table 1. Informational data on the monoenergetic neutron fields at PTB.

Figure 4: Picture of the experimental set-up in the low-scattering measurement hall at PTB. Target-to-detector distance is indicated by the red line.

Detectors numbers	MS number	t (s)	ϕ_{dir} (10^5 cm^{-2}
#100413 / #100497	4	299.6	0.80(4)
#100413 / #100497	5	308.6	0.84(4)
#100413 / #100497	6	316.7	0.86(4)
#100413 / #100497	7	298.3	0.80(3)
#100508 / #100520	8	896.7	2.41(10)
#100508 / #100520	9	630.7	1.70(7)
#100508 / #100520	10	51.8	0.140(6)
#100508 / #100520	11	601.0	1.62(7)
#100508 / #100520	12	410.9	1.11(5)
#100508 / #100520	13	522.1	1.41(6)

Table 2. Measurement time duration and direct neutron fluence rate for irradiation tests with a monoenergetic 2.5 MeV neutron field.

a distance of 300 cm from the neutron generator. The detectors were supported and enclosed by foamed material, and the distance from the detectors to the neutron production target was measured along the direction of the ion beam between the plane containing the axis of the detector housings and the neutron production target. The direction of the ion beam hits this plane in the middle between the centers of the sensitive volumes. The experimental set-up is shown in Figure 4.

Table 1 shows informational data on the monoenergetic neutron fields, such as the type of nuclear reaction exploited to generate the neutron field, nominal values of neutron energies and FWHMs of the irradiation fields.

In Table 1, the neutron emission angle θ_n, the neutron field energy E_n, and the width ΔE_n (FWHM) of the direct neutron distribution are nominal values. Standard measurement uncertainties (k = 1) are given for the ratio ($\varnothing_{sc}/\varnothing_{dir}$) of the fluence values of scattered and direct neutrons. As for the measured neutron fluence values that were used as a reference for each irradiation field, the related uncertainties are expanded measurement uncertainties obtained by multiplying the standard measurement uncertainties by a coverage factor (k = 2). They have been

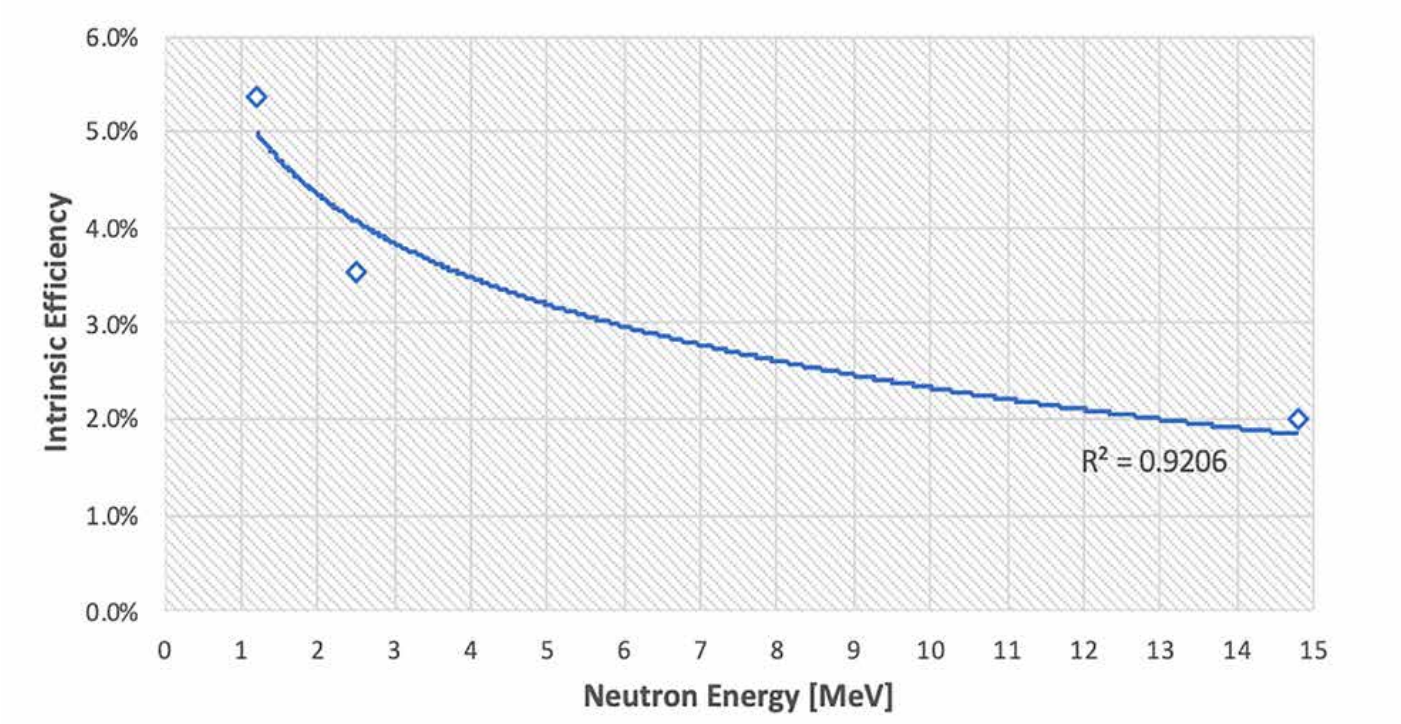

Figure 5: Intrinsic efficiency values calculated for 1.2, 2.5, 14.8 MeV neutron energies, together with the analytical fit.

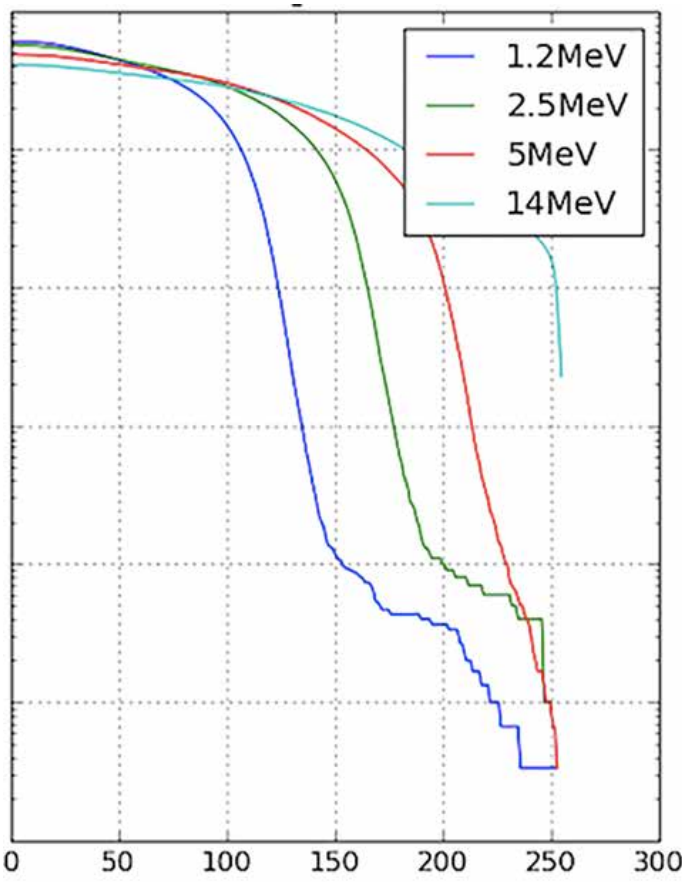

Figure 6: Detector response to various monoenergetic neutron fields in terms of cumulative count rate versus ToT channel.

determined in accordance with the Guide to the Expression of Uncertainty in Measurement (GUM) [7]. The value of the measurand then normally lies, with a probability of 95%, within the attributed coverage interval.

These neutron fluence measured values, together with the time duration of the test and the generator-to-detector distance, were used to calculate the neutron fluence rate at the detector surface in units of $cm^{-2}s^{-1}$.

For each measurement performed with the s670 neutron detector, the detector output is a histogram in which for every event generating a signal that is above the offset, a count is stored in a histogram and distributed over 255 ToT channels depending on the amplitude of the light pulse generated by that event. By summing over all the counts above the low-cut (set to achieve the desired gamma-immunity) and dividing by the measurement time duration, the measurement count rate is calculated for each irradiation energy. By subtraction of the background count rate, the net neutron count rate has been calculated for all the irradiation tests.

Moreover, by multiplying the neutron fluence rate at the detector surface by the sensitive cross-sectional area of the tube, the number of neutrons hitting the detector per unit time was calculated.

From the ratio between the net neutron count rate and the number of neutrons hitting the detector per unit time, the intrinsic efficiency of the detector was calculated for all the irradiation energies.

In Table 2 the reference neutron fluence values and irradiation time for the 2.5 MeV irradiation tests are shown as an example.

3.2 Intrinsic efficiency assessment and energy calibration

The intrinsic efficiency values calculated for energies of 1.2, 2.5 and 14.8 MeV are plotted in figure 5, where the analytical fit is shown as well.

This analytical fit was then used when implementing the dose rate calibration in the system software, in order to calculate the neutron fluence rate from the detector count rate for neutron energies in this range.

In Figure 6, the response of the s670 detector to irradiation energies of 1.2, 2.5, 5.0 and 14.8 MeV are shown in terms of the cumulative count rate versus ToT channel.

The response curves are clearly characterised by an increasing cut-off ToT channel number with increasing irradiation energy. The positions of these cut-off points were then used to calibrate in energy the ToT histograms in order to have direct information about the neutron field energy out of a measurement histogram.

From the physics of the elastic scattering interaction between a neutron and a helium nucleus, it is easily calculated that a neutron can deposit up to 64% of its initial kinetic energy to the target nucleus [3].

Thus, it is straightforward to associate the maximum deposited energy (and then the initial neutron energy) to the ToT channel where the irradiation of the detector with a field of that energy would show a cut-off. The energy calibration points, and the related analytical fit implemented into the system software are shown in the graph in figure 7.

Neutrons effective dose per fluence factors (in units of pSv cm^{-2}) from ICRP Publication 116 (Table A.5, mono-energetic particles incident in various geometries) were used to implement the dose rate calculation in the system software [4]. For each energy region resulting from the ToT histograms calibration, a set of neutron effective dose per fluence factors was used to estimate the dose rate delivered by neutrons belonging to that region.

After the implementation of this dose-rate calculation in the detector software, the final tests were performed at Paul Scherrer Institut (PSI) Calibration Laboratory [6]. A

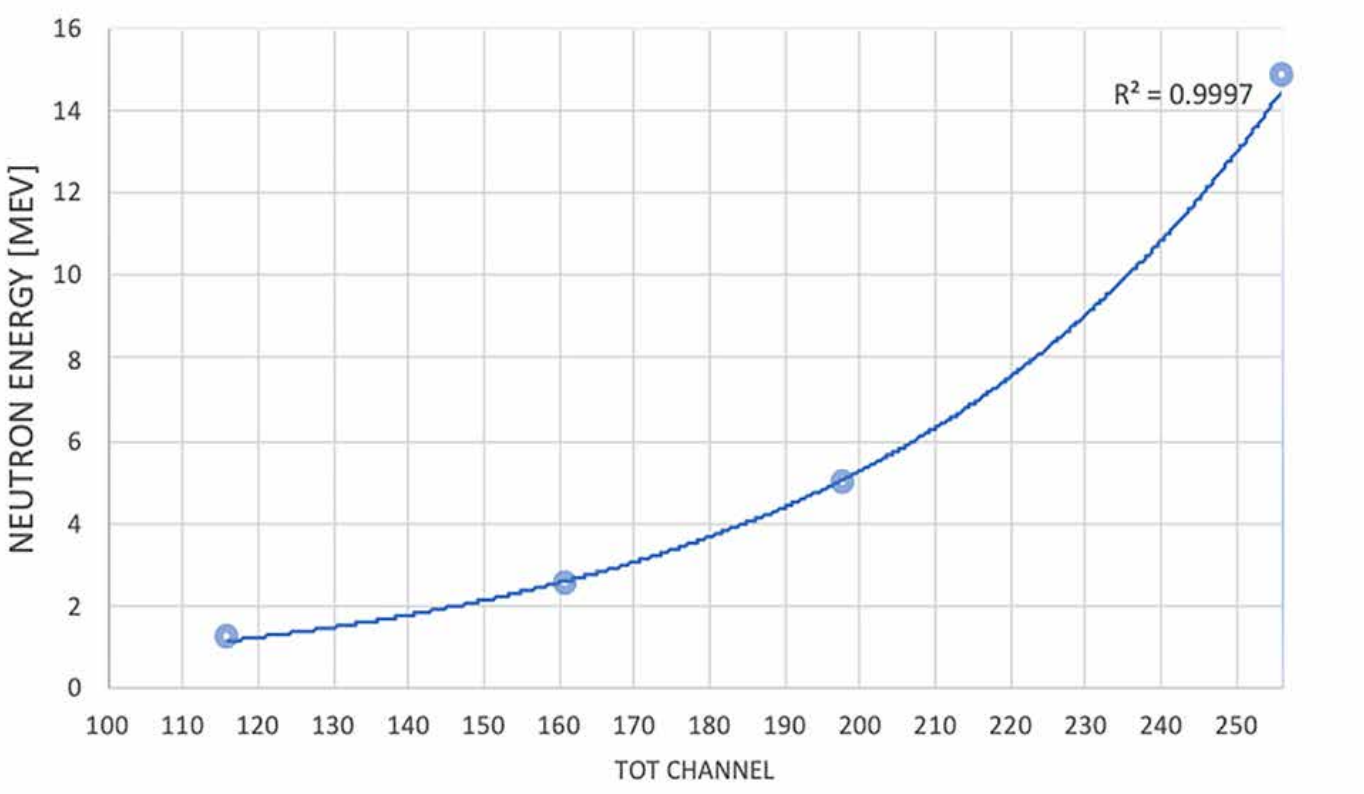

Figure 7: Energy Calibration points and analytical fit in the energy range 1.2 – 14.8 MeV..

spontaneous fission ^{252}Cf and an alpha-neutron ^{241}Am—Be source were used.

Characteristics of these neutron sources are shown in Table 3.

The PSI Calibration Lab uses a Berthold LB6411 neutron detector with an UMO LB 123 neutron dosimeter as a secondary standard. The expanded combined uncertainty (k = 2) of the dose rate values used as reference was estimated by PSI to be 6% for ^{252}Cf and 7-8% for ^{241}Am-Be for distances larger than 50 cm. Higher uncertainty for ^{241}Am-Be is due to the uncertainty of a field-specific correction factor to the calibration of the secondary standard LB6411, which was calibrated in a direct neutron field from a ^{252}Cf source.

Nuclide	^{241}Am-Be	^{252}Cf
Nominal Activity [GBq]	185	19.68
Neutron source strength [n/s]	9.15E+06	2.29E+09
Reference Date	10.10.59	05.12.01

Table 3. Characteristics of the neutron sources used at PSI Calibration Laboratory [5].

4. Results

Defining the Response Factor (RF) as the ratio between the measured ambient dose rate value at distance d from the source and the reference ambient dose rate value at the same distance certified by PSI for each source, the detector performance was evaluated for both sources at various source-to-detector distances and for various measurement duration. Two s670 detectors were irradiated (serial numbers 100488 and 100509, as shown in Table 4).

The acceptance range for the Response Factor is set as to have a maximum error of +/- 20% with respect to the dose rate value declared by PSI. Results of the ambient dose equivalent rate measurements for these two sources are shown in Table 3 for source-to-detector distances of 1 m and 3 m and measurement duration of 60 s and 10 s. The measurement at 3 m with duration of 10 s is shown to represent the worst-case scenario for this fixed source activities and measurement setup.

5. Conclusions

The results presented in Table 4 show that the accuracy of the dose rate calculation is inside the defined acceptance range for both sources and for different source-to-detector distances and durations of the measurements, giving an overall average accuracy of 92.5% calculated over all the

distance = 1m; duration 60s	Reference H*(10) [uSv/h]	100488 [uSv/h]	100488 RF [0.8-1.2]	100509 [uSv/h]	100509 RF [0.8-1.2]	100488 Calib.	100509 Calib.
AmBe	115.2	106.5	0.92	127.2	1.10	passed	passed
Cf-252	222.3	217.9	0.98	247.4	1.11	passed	passed

distance = 3m; duration 60s	Reference H*(10) [uSv/h]	100488 [uSv/h]	100488 RF [0.8-1.2]	100509 [uSv/h]	100509 RF [0.8-1.2]	100488 Calib.	100509 Calib.
AmBe	20.2	17.2	0.85	19.4	0.96	passed	passed
Cf-252	38.2	35.6	0.93	40.0	1.05	passed	passed

distance = 1m; duration 10s	Reference H*(10) [uSv/h]	100488 [uSv/h]	100488 RF [0.8-1.2]	100509 [uSv/h]	100509 RF [0.8-1.2]	100488 Calib.	100509 Calib.
AmBe	115.2	105.1	0.91	125.6	1.09	passed	passed
Cf-252	222.3	223.0	1.00	238.9	1.07	passed	passed

distance = 3m; duration 10s	Reference H*(10) [uSv/h]	100488 [uSv/h]	100488 RF [0.8-1.2]	100509 [uSv/h]	100509 RF [0.8-1.2]	100488 Calib.	100509 Calib.
AmBe	20.2	17.8	0.88	21.7	1.07	passed	passed
Cf-252	38.2	36.1	0.94	40.1	1.05	passed	passed

Table 4: Results of the dose rate measurements with radionuclide neutron sources at PSI for the s670 neutron detectors #100488 and #100509

measurements shown in Table 4. This clearly shows how this fast neutron detection system can serve as a neutron dose meter for radiological safety purposes in environments where neutron dose rate of neutron fluxes in the fission energy range must be constantly monitored, such as nuclear power plants, fuel reprocessing facilities and nuclear waste analysis laboratories. The National Institute of Metrology of China (NIM) certified the first s670 fast neutron detector as a neutron dose meter in China in 2020. Avoiding the use of helium-3 and the employment of large volumes of moderating material, the s670 fast neutron detector can represent a robust, compact and versatile alternative to these detectors, with the additional feature of providing an accurate dose rate calculation for fast neutrons in the fission energy range.

References

[1] R. Chandra et al. Fast neutron detection with pressurized 4He scintillation detectors. JINST 7 C03035. 2012.

[2] Murer D.E. He-4 Fast Neutron Detectors in Nuclear Security Applications. ETH Zürich. 2014.

[3] Knoll G. F. Radiation Detection and Measurements, 4th Ed.

[4] Conversion Coefficients for Radiological Protection Quantities for External Radiation Exposures. Table A.5. ICRP Publication 116, Ann. ICRP 40(2–5). 2010.

[5] URL: https://www.ptb.de/cms/en/ptb/fachabteilungen/abt6/measurement-and-calibration-capabilities/neutron-radiation.html

[6] URL: https://www.psi.ch/de/asi/facilities

[7] International Organization for Standardization (ISO). Evaluation of measurement data. Guide to the expression of uncertainty in measurement. JCGM 100:2008.